PCCP

Accepted Manuscript

This is an *Accepted Manuscript*, which has been through the Royal Society of Chemistry peer review process and has been accepted for publication.

Accepted Manuscripts are published online shortly after acceptance, before technical editing, formatting and proof reading. Using this free service, authors can make their results available to the community, in citable form, before we publish the edited article. We will replace this *Accepted Manuscript* with the edited and formatted *Advance Article* as soon as it is available.

You can find more information about *Accepted Manuscripts* in the Information for Authors.

Please note that technical editing may introduce minor changes to the text and/or graphics, which may alter content. The journal's standard Terms & Conditions and the Ethical guidelines still apply. In no event shall the Royal Society of Chemistry be held responsible for any errors or omissions in this *Accepted Manuscript* or any consequences arising from the use of any information it contains.

ARTICLE TYPE

Photo-thermal effects in gold nanoparticles dispersed in thermotropic nematic liquid crystals†

Luigia Pezzi,*[a] Luciano De Sio,[b] Alessandro Veltri,[c] Tiziana Placido, [d,e] Giovanna Palermo, [a] Roberto Comparelli, [e] Maria Lucia Curri, [e] Angela Agostiano, [d,e] Nelson Tabiryan [b] and Cesare Umeton [a]

The last years have seen a growing interest in the ability of metallic nanoparticles (MNPs) to control temperature at the nanoscale. Under a suitable optical radiation, MNPs feature an enhanced light absorption/scattering, thus turning into an ideal nano-source of heat, remotely controllable by means of light. In this framework, we report our recent efforts on modeling and characterizing the photo-thermal effects observed in gold nanoparticles (GNPs) dispersed in thermotropic Liquid Crystals (LCs). The photo-induced temperature variations in GNPs dispersed in Nematic LCs (NLCs) have been studied by implementing an ad hoc theoretical model based on the thermal heating equation applied to an anisotropic medium. Theoretical predictions have been verified by performing photo-heating experiments on a sample containing a small percentage of GNPs dispersed in NLC. Both theory and experiments represent an important achievement in understanding the physics of heat transfer at the nanoscale, with applications ranging from photonics to nanomedicine.

1 Introduction

Nanophotonics concerns the study of the interaction between light and nanosized objects, and involves many research fields such as physics, chemistry, biology, nanomedicine. Plasmonics is a field of nanophotonics that studies the interactions between electromagnetic field and free electrons in a metal nanoparticle, as they can be excited by the electric component of light to undergo collective oscillations, that are plasmons. In this framework, metallic nanoparticles (MNPs) have the intrinsic ability to confine light at the nanoscale trough the excitation of the Localized Plasmonic Resonance (LPR), a phenomenon related to the oscillation of the free electrons localized at the metal/dielectric interface. Under a resonant light illumination, MNPs convert light into heat, thus becoming nanosources of heat and opening up an unpredictable number of applications, ranging from photonics to nanomedicine[1–4]. This occurs because the absorption associated to the LPR triggers a heat generation process that involves not only absorption of incident photons, but also heat transfer from the MNPs to the surrounding medium. Gold nanoparticles (GNPs) have gained an important role because their LPR can be tuned from the visible to the near-infrared (NIR) range by simply changing size, shape, or dielectric function of the surrounding medium. Moreover, GNPs are bio-compatible and can be easily functionalized with a large variety of molecules, exhibiting also a weak oxidation. Thanks to these properties, GNPs have been widely exploited in cancer therapy[5–9], ophthalmology and dermatology, nanosurgery[10,11], photothermal drug delivery and gene therapy[12–14], photothermal imaging[15], plasmon-assisted nanochemistry[16], plasmon-assisted optofluidics[17] and sensing[18,19]. Monitoring nanoscale temperature variations in samples under optical illumination represents, therefore, an important issue not only for nanomedicine but also for photonics and plasmonics. Direct temperature measurements have been made by means of thermal camera analysis[20] with high sensitivity ($\approx 0.2^oC$); the technique possesses, however, a limited spatial resolution ($10-15\mu m$), enabling only for a surface measurement of temperature. So far, approaches, based on combination of GNPs and phase transitions, generally require embedding the GNPs in ice[21] or employing suspensions of GNPs in organic solvents[22]; these techniques can hardly combine the advantages of reliability, fast readout rate and high-resolution, thus limiting their util-

[a] *LICRYL (Liquid Crystals Laboratory), Department of Physics University of Calabria, 87036 Arcavacata di Rende (CS), Italy. Fax: XX XXXX XXXX; Tel: +39 0984 496147; E-mail: luigia.pezzi@fis.unical.it*
[b] *Beam Engineering for Advanced Measurements Company, Winter Park, Florida 32789, USA.*
[c] *Colegio de Ciencias e Ingeniera, Universidad San Francisco de Quito, Quito, Ecuador.*
[d] *Università degli Studi di Bari Dip. Chimica, Via Orabona 4, 70126 - Bari, Italy.*
[e] *CNR-IPCF Istituto per i Processi Chimici e Fisici, Sez. Bari, c/o Dip. Chimica Via Orabona 4, 70126 - Bari, Italy.*

ity for nanoscale temperature monitoring. In this perspective, an original approach has been presented for monitoring nanoscale temperature variations in GNPs under optical illumination, which is based on a combination of gold nanorods (GNRs) and chiral thermotropic liquid crystals (CLCs)[23,24]. Such a combination allows to measure temperature around GNRs, after a given illumination time, with a sensitivity of about 0.03^oC. However, the heat transfer mechanism from the hot GNRs to the CLCs remains still mostly unexplored, since modeling GNRs and CLCs, that can be seen as twisted structures (just like in a spring), requires complex theoretical models/numerical simulations. In this paper, a simplified approach to describe the combination of spherical GNPs and NLCs is presented. By exploiting the symmetry of spheres (GNPs) and the unidirectional order of Nematic LCs (NLCs), we have realized a theoretical model along with an experimental investigation to specifically study the heat generation and its transfer mechanism from the photo-heated GNPs to the surrounding medium (NLC).

2 Theoretical model

When a light beam of suitable wavelength impinges on a GNP the electrons of its conductive band start to oscillate coherently with the electric field of the impinging light. This phenomenon results in a strong absorption (the so called LPR) that is responsible for the heat production. In the absence of phase transitions, in order to predict the temperature around a GNP it is necessary to solve the heat transfer equation (Eq. 1), which derives from a balance of heat energy: the net rate of thermal energy that comes out from the GNP, plus the rate of thermal energy accumulation (internal energy variation in the GNP) must equal the net rate of thermal energy generation

$$\nabla \cdot (-k(\mathbf{r})\nabla T(\mathbf{r},t)) + \rho(\mathbf{r})c(\mathbf{r})\frac{\partial T(\mathbf{r},t)}{\partial t} = Q(\mathbf{r},t) \quad (1)$$

where $\mathbf{r}$ and t are the spatial and time coordinates, $T(\mathbf{r},t)$ is the local temperature and parameters $k(\mathbf{r})$, $\rho(\mathbf{r})$, $c(\mathbf{r})$ indicate thermal conductivity, mass density and specific heat, respectively. The function $Q(\mathbf{r},t)$ represents the energy source coming from the energy dissipation inside GNPs. At the thermal equilibrium the solution of the Eq. (1) is obtained by taking into account a heat production Q at a constant rate per unit time and per unit volume inside the spherical NP (distance $0 \leq r \leq R_{NP}$ and conductivity K_0) while in the region $r > R_{NP}$ the conductivity of the host medium is K_H and no heat production occurs[25]. Calculations yield a temperature variation

$$\Delta T = \frac{QR_{NP}^3}{3rK_H} \quad (2)$$

where the thermal energy generation Q is

$$Q = <\mathbf{J}(\mathbf{r},t) \cdot \mathbf{E}(\mathbf{r},t)>_t = \frac{\varepsilon_0 \omega \mathfrak{I}[\chi_{NP}]|\mathbf{E}_{int}|^2}{2} \quad (3)$$

and depends on the electric field $\mathbf{E}_{int}$ inside the GNP and on the imaginary part of dielectric permeability $\mathfrak{I}[\chi_{NP}]$ (that describes energy dissipation of the GNP, or dielectric losses); ω is the angular frequency of light and ε_0 is the dielectric permittivity of vacuum.

The Mie theory[26] provides the expression for the electric field $\mathbf{E}_{int}$ inside a spherical GNP. However, in our case the average size of the used GNPs ($r = 10\,nm$) is much smaller than the used wavelength ($\lambda = 532\,nm$), a circumstance that allows us to use the following quasi-static formula:

$$\mathbf{E}_{int} = \frac{3\varepsilon_H}{2\varepsilon_H + \varepsilon_{NP}}\mathbf{E}_0 \quad (4)$$

where ε_{NP} is the dielectric permittivity of the spherical GNP, ε_H the dielectric permittivity of the host medium and $\mathbf{E}_0$ the amplitude of the applied electric field. Then, the resonance of the GNP correspond to the maximum of the thermal energy production with a temperature variation given by:

$$\Delta T = \frac{V_{NP}}{2k_H\lambda r}\frac{\mathfrak{I}[\chi_{NP}]}{\sqrt{\varepsilon_H}}\left|\frac{3\varepsilon_H}{2\varepsilon_H + \varepsilon_{NP}}\right|^2 I_0 \quad (5)$$

where V_{NP} is the GNP volume, λ the wavelength of light, r the distance from the NP and I_0 the intensity of the impinging light (gaussian beam)[27]. For instance, Equation (5) can be used to predict the temperature variation around GNPs in water under optical illumination, where it is possible to assume no refractive index change with temperature[2] variation.

In our case, we have both developed a theoretical model and carried out an experimental characterization by considering spherical GNPs dispersed in a well known and commercially available thermotropic NLC (E7, by Merck)[28].
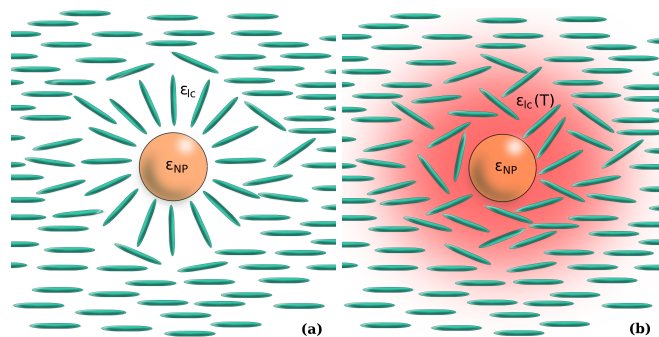

Fig. 1 Sketch of the GNP dispersed in NLC: (a) without heating, (b) with heating

In order to study such a complex system, knowledge of the optical properties of the single constituents is required.

NLCs are elastic and anisotropic materials that possess both dielectric[29–33] and thermal conductivity[34] dispersion. Moreover, their optical properties (e.g. birefringence) can depend on different external parameters, such as wavelength of the impinging radiation, external electric fields, and temperature. In particular, the wavelength and temperature dependence of their refractive indices (both ordinary and extraordinary) are described by the extended Cauchy equations[31]:

$$n_e(\lambda, T) = n_i(\lambda) + G'(\lambda)S(T) \quad (6)$$

$$n_o(\lambda, T) = n_i(\lambda) - \frac{G'(\lambda)S(T)}{2} \quad (7)$$

$$\Delta n(\lambda, T) = \frac{3G'(\lambda)S(T)}{2} \quad (8)$$

where $n_i(\lambda)$ is the refractive index of the isotropic state, n_o and n_e are the ordinary and extraordinary indices of the NLC respectively, $G'(\lambda)$ is a proportionality constant (insensitive to temperature) and $S(T)$ is the order parameter of the NLC. By using typical (experimental) values of the E7 NLC in Eq.(8)[33], it is possible to obtain the expressions for both n_o and n_e as a function of temperature and wavelength of the impinging radiation.
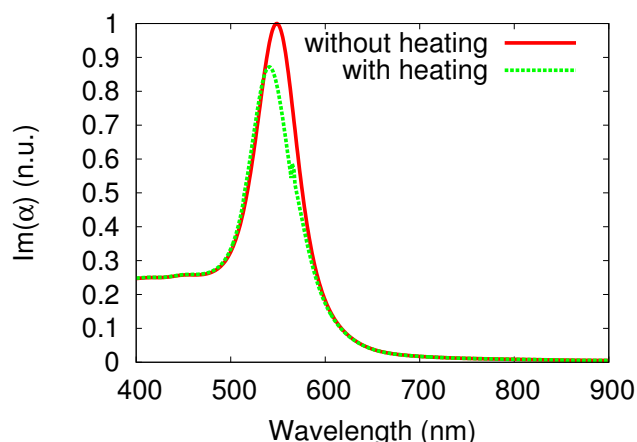

Fig. 2 Imaginary part of the polarizability of the system (GNP + NLC) as a function of wavelength of the impinging radiation.

As for GNPs, an impinging resonant radiation induces an electrical current due to the onset of the LPR; then the Joule heating effect produces a temperature increase in each GNP. Consequently, this cools down by exchanging heat with the surrounding medium (NLC), which undergoes a dielectric permittivity variation, thus affecting the temperature variation of the GNP. We have implemented a numerical simulation in order to estimate both the equilibrium temperature of the system and the variation of the refractive indices of the NLC (surrounding medium). The modeled system is made of a single spherical GNP immersed in NLC (Fig. 1). By fitting the experimental values reported in ref.[33] it is possible to obtain the Cauchy coefficients[30–33]. These coefficients provide an equation both for n_e and n_o as functions of T and λ, that can be easily implemented by using our numerical code. The equilibrium temperature of our system has been obtained by using Eq. 5 and realizing a do-while loop with the Eq. 6 (the loop is closed every time ΔT is less than 0.1^oC).

The polarizability α of the particle can be expressed as $\alpha = 3V_{NP}(\varepsilon_{NP} - \varepsilon_{LC})/(\varepsilon_{NP} + 2\varepsilon_{LC})$, where ε_{NP} is the dielectric permittivity of the GNP, V_{NP} is its volume, and ε_{LC} is the permittivity of the NLC. It is easy to show that α is directly related to the absorption cross section (C_{abs}) trough to the equation $C_{abs} = k\Im[\alpha]$ where k is the thermal conductivity of gold. Fig. 2 reports the calculation of the imaginary part of the polarizability as a function of the impinging radiation wavelength in two cases: the blue curve has been obtained by considering that the refractive index of the surrounding medium does not change due to heating (e.g. external pump beam Off); the green curve, represents the polarizability of the system when the NLC refractive index changes because of the heating (e.g. external pump beam On). In both cases, the two curves exhibit a quasi-Lorenzian lineshape which is very similar to the absorption spectrum of monodispersed GNPs (see experimental part for details). The observed blue shift can be explained by taking into account that the resonance condition is fulfilled (Fröhlich condition) if $\Re[\varepsilon_{NP}(\omega)] = -2\varepsilon_{LC}$. A modification in the value of the dielectric constant of the host material corresponds, therefore, to a tuning action on the LPR frequency. In our case, due to a heat induced decreasing of ε_{LC}, the Fröhlich condition is fulfilled for higher (negative) values of ε_{NP}. It is well known[35] that, in the visible range, the real part of the electric permittivity of GNPs increases with frequency; therefore, fulfillment of the Fröhlich condition takes place for higher values of ω. This yields a blue shift of the plasmonic absorption peak. Fig. 3 shows a map of the dielectric anisotropy $\Delta n = n_e - n_o$ vesus the impinging light wavelength and intensity. The dark area highlights that a remarkable variation of Δn occurs only nearby the LPR frequency, where the absorption (see Fig. 2) and, therefore, the temperature variation of the system exhibit their maximum. All above reported theoretical predictions have been validated by means of an experimental analysis reported in the next section.

3 Experimental results

Spherical cetyltrimethylammonium chloride (CTAC)-capped GNPs have been synthesized in aqueous solution and subsequently transferred in chloroform, which is a solvent (dispersing medium) also for Liquid Crystals (LCs). The general protocol for seed-mediated synthesis of GNPs and their transfer
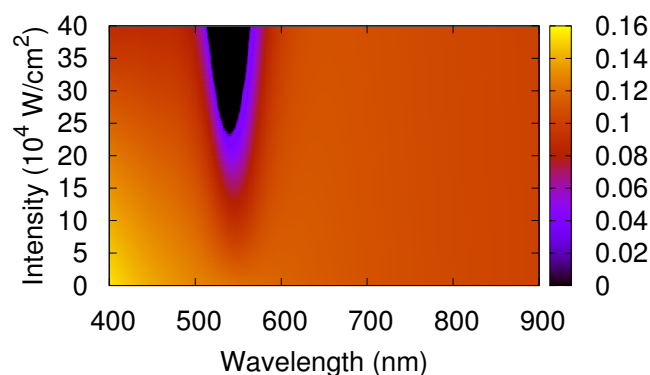
Fig. 3 Map of the NLC birefringence as a function of light wavelength and intensity.

Fig. 4 UV-vis absorption spectrum of GNPs dispersed in chloroform and their TEM image (inset).

from water to chloroform is described in details in the *supporting information* section. Such an approach makes GNPs stabilized in aqueous solution thanks to the bilayer of CTAC surfactant capping the particles, thus conferring them surface positive charge. GNPs can be successfully extracted into the organic phase by decanoic acid, which electrostatically binds the CTAC bilayer by means of deprotonated carboxylic group in basic pH conditions; the alkylic group, on the other side, makes GNPs dispersible in chloroform[24]. GNPs have been characterized by means of UV-vis absorption spectroscopy in the $400 - 800\,nm$ range: their absorption spectrum, after the phase transfer in organic medium is reported in Fig. 4 and shows the typical LPR band centered at $526\,nm$. Transmission Electron Microscope (TEM) analysis has been performed by a Jeol JEM-1011 microscope operating at $100\,kV$. The specimens have been prepared by depositing a drop of the GNPs dispersion onto a carbon-coated copper grid and then allowing the solvent to evaporate. For a statistical determination of the average GNP size, at least 200 objects have been counted. The TEM image of GNPs, shown in Fig. (4) (inset), confirms that the particle population consists of GNPs with $17.4 \pm 2.2\,nm$ diameter; size and shape remain unchanged after phase transfer from the aqueous to the organic medium. Homogeneous mixtures of GNPs up to 6% in weight in NLC (MDA-00-1444, by Licristal) have been obtained; however, above 4wt.%, the order parameter of the NLC phase is affected by the presence of GNPs as shown by a dramatic drop of the birefringence value. For this reason, we have used the mixture with the highest concentration of GNPs (3 wt.%) which does not affect the NLC phase. ITO coated glass substrates have been treated with a polyimide layer and rubbed for obtaining a planar orientation of the NLC director. A cell with a $2.7\,\mu m$ cell gap has been filled with the NLC/GNPs mixture by capillary action at room
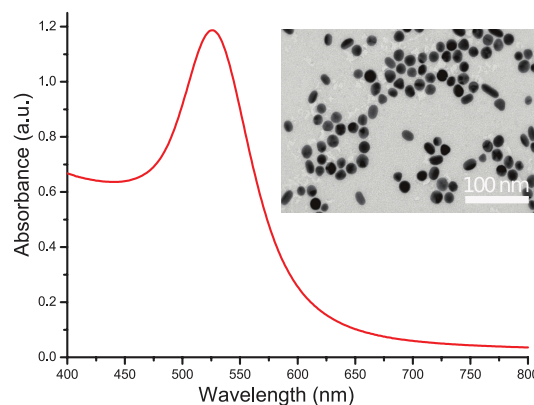
temperature; the NLC director oriented parallel to the substrates along the rubbing direction (see red arrow in Fig. 5a). The excellent optical quality of the sample is evident in the polarizing optical photographs shown in Fig. 5. The optical con-
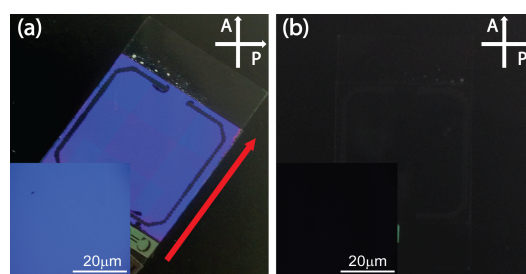

Fig. 5 Pictures of the sample between crossed polarizers (a, b) along with their POM view. The director of the NLC is aligned at 45° in (a) and at 0° in (b). The red arrow represents the rubbing direction.

trast between bright (Fig. 5a) and dark (Fig. 5b) states is higher than $40:1$ for white non collimated light, and indicates an excellent NLC alignment. To check the spatial uniformity of this alignment, we have performed optical observations by means of a Polarized Optical Microscope (POM) equipped with a CCD color camera connected to a PC; results are reported in the insets of Fig. 5(a, b). The uniform change in contrast of the whole area (from Fig. 5a to Fig. 5b) suggests the NLC director alignment has not been macroscopically affected by the presence of GNPs, which are well dispersed in the NLC. Indeed, no NLC defects are visible in the POM view of the sample (insets of Fig. 5(a, b)). It is worth mentioning that, due to the low concentration (3 wt.%) of GNPs dispersed in the thin ($2.7\,\mu m$) NLC layer, the spectral analysis of the sample did not show any observable absorption peak (LPR) related to the presence of the GNPs. However, the spectral analysis (not shown here) performed on the vial of GNPs/NLC mixture exhibits the same behavior reported Fig. 2. Experiments devoted

to investigate the influence, on the NLC director alignment, of the local heating induced by a suitable optical radiation (trough the GNPs resonance) have been performed by using the all-optical setup reported in Fig. 6. The system used a low
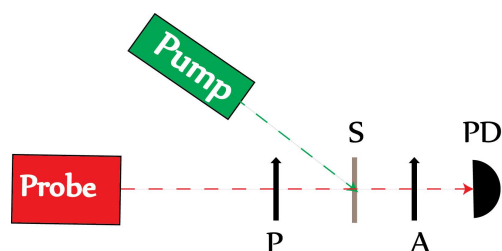

Fig. 6 All-optical setup for sample characterization. P: polarizer; S: sample; A: analyzer; PD: photodetector.

power density ($P_{probe} = 0.2 W/cm^2$) CW probe laser, emitting at $\lambda = 633 nm$ and a CW pump laser emitting at $\lambda = 532 nm$, in the high absorption spectral range of GNPs (Fig. 4). For sake of simplicity, an unfocused pump beam, which impinges on the sample with an oval shape of about $(2 \times 3) mm^2$, has been used. The photo-thermal response of the sample has been observed between crossed polarizers, with the optical axis of the sample (NLC director orientation) set at 45° with respect to the polarizer/analyzer axes. Under this condition, the sample acts as a retardation plate and the transmitted intensity can be detected by a photo-detector. Fig. 7a reports the probe intensity transmitted by the system, detected for different values of the pump light intensity (from $0.4 W/cm^2$ to $3.1 W/cm^2$, probe power kept constant). By optically pumping the same probed sample area, the photoexcitation of GNPs induces an electric-driven Joule heating, with a consequent energy exchange with the surrounding NLC. Such a local-heating induces a gradual suppression of the transmitted intensity, which is due to an induced reduction of the birefringence (Δn) of the sample. In fact, this has been calculated by using the Jones matrix formalism and exploiting the contrast between the steady state intensity transmitted by the sample with its optical axis at 45° with the crossed polarizers, and the steady state intensity transmitted by the sample with its optical axis at $0^o/90^o$ with the crossed polarizers[36]. Fig. 7b shows that Δn values vary from 0.135 down to almost zero. The initial value of Δn is lower than in the pure NLC ($\Delta n \approx 0.2$); this can be explained by taking into account that the NLC order parameter is affected by the presence of GNPs, which may act as impurities, thus locally modifying (at the molecular scale) the NLC molecules order. It is worth noting that pump-probe experiments (not reported here) performed on a "reference" pure NLC cell of the same thickness, show that no variations in the trasmitted probe intensity are detected, neither when the sample is acted on by the highest intensity pump beam ($3.1 W/cm^2$).

We have also performed a control experiment by detect-

ing, as a function of the sample temperature, the transmittance of both the "reference" pure NLC cell, and our NLC/GNPs cell placed (inside a hot stage) between crossed polarizers, with the optical axis of the sample set at 45° with the polarizer/analyzer axes. In both cases, as the sample temperature was increased, the transmitted intensity decreased towards a minimum which is almost zero. In addition, curves show that, in the reference cell, the pure NLC undergoes transition from nematic to isotropic at about 65^oC; on the other hand, in the cell containing NLC and dispersed GNPs, these ones act as a destabilizer perturbation for the NLC, lowering its transition temperature of about 10^oC, from about 65^oC to about 55^oC (see supporting information). Fig. 7c shows the Δn behavior
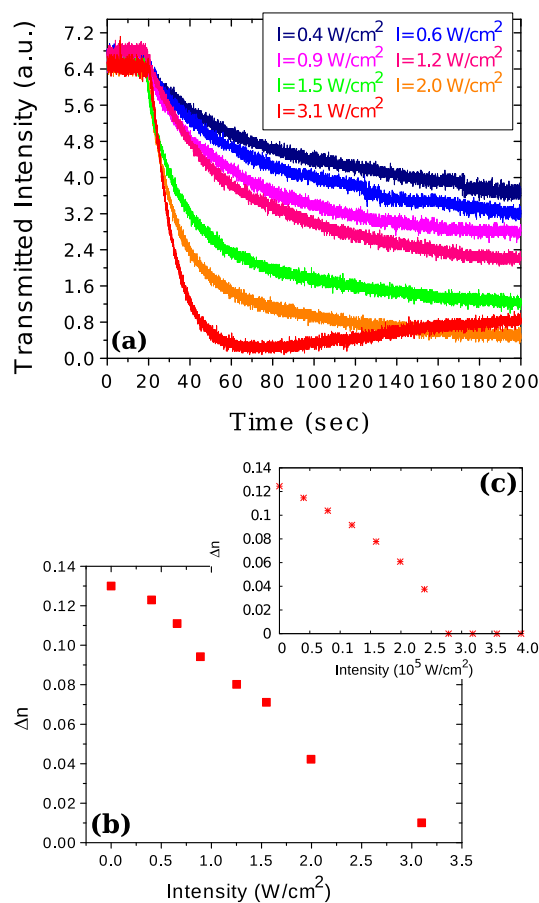

Fig. 7 Transmitted intensity versus time for different intensity values of the pump radiation (a). Birefringence of the sample versus the intensity of the pump radiation ($\lambda = 532 nm$) (b); calculated birefringence versus the intensity radiation for a specific wavelength ($\lambda = 532 nm$) (c).

predicted by our theoretical model: both experimental and theoretical results qualitatively exhibit the same behavior, while, from a quantitative point of view there is a discrepancy between the experimental and the theoretical photo-heating in-

tensity needed to induce the observed effect. A detailed analysis of this aspect is discussed in the next section. From curves of Fig. 7 it is clear that, starting from $3.1 W/cm^2$, new phenomena take place, that are related to a nonlinear response of the liquid crystal and give rise to effect that are preeminent with respect to the thermal one. At higher enough intensities, the transition of the LC to the isotropic phase takes place and the transmittance becomes zero. Those effects evolve with longer timescales and are out of the interest of the present work [37,38]. To validate our model and verify that the NLC does not play
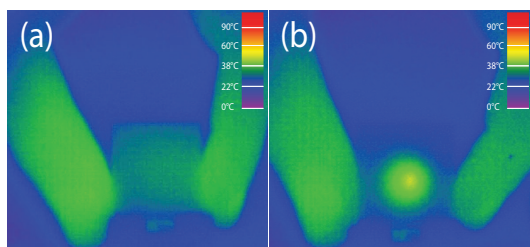
Fig. 8 Thermographic analysis of the sample under optical irradiation for the pure NLC (a) and NLC/GNPs (b) cell.

any role in the photo-heating conversion, we have performed a control experiment by fabricating a sample made of pure NLC. The comparison has been performed by means of a thermographic analysis (thermocamera sensitivity $\approx 0.5^oC$) both of pure NLC and NLC/GNPs samples, under optical illumination. Experiments have been realized by keeping operator's hand fingers ($T \approx 37^oC$) close to the sample, in order to have a comparison setpoint: Fig. 8a shows that the thermocamera does not detect any color change (that is temperature variation) for the pure NLC sample ($I = 3.1 W/cm^2$; illumination time$= 300 s$). On the contrary, in the same experimental condition, the thermographic analysis realized on the GNPs/NLC sample (Fig. 8b) shows that the surface of the illuminated area has been heated at a temperature of about 60^oC (close to the nematic to isotropic transition of the NLC), meanwhile the setpoint is kept at almost the same previous temperature ($T \approx 37^oC$). This result is an incontrovertible experimental evidence that the photo-heating process is due to the photoexcitation of GNPs, with a consequent heat exchange with the surrounding NLC medium.

Finally, we have studied the dynamics of the system. A switching behavior which turns out to be reversible and repeatable, is observed when a sequence of pump beam pulses, obtained by utilizing an electronic shutter, is allowed to impinge onto the sample, put between crossed polarizers, with its optical axis forming an angle of 45° both with the polarizer and the analyzer axes. Fig. 9 shows that, when the pump is switched on ($I = 3.1 W/cm^2$), a photoexcitation of GNPs occurs, with a consequent phase transition of the NLC from the nematic to the isotropic state; thus between crossed polarizers
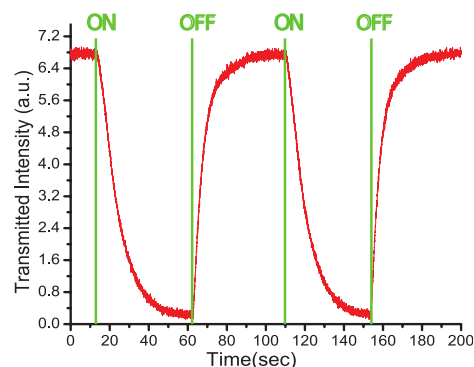
Fig. 9 Switching behavior observed by using a periodic sequence of pump beam pulses. ON and OFF refer to the pump beam being allowed to impinge on the sample or not.

the probe light experiences just the isotropic refractive index ($n_{iso} = 1.56$) of the NLC, and the transmitted intensity drops to zero ($\tau_{on-off} = 40 s$). When the green pump beam is switched off, the NLC cools down and the Isotropic to Nematic transition occurs, thus restoring the sample birefringence, and, therefore, a transmitted light intensity ($\tau_{off-on} = 20 s$).

4 Discussion

Despite the good qualitative agreement between theoretical predictions and experimental results, (Fig. 7b-c), we have noted that, in the experiments, the photo-heating of the NLC has been obtained with a resonant intensity value ($3.1 W/cm^2$) that is quite lower than the one predicted by the theoretical analysis, a discrepancy already reported in previous studies by Baffou and Govorov [1–4]. In the latter case, the authors have studied plasmonic photo-heating in a system made of GNPs dispersed in water/ice, observing that the photo-induced heat occurs with an energy flow (intensity) which is several orders of magnitude lower than the one predicted by their simulations. Looking at the energy balance already discussed in the theoretical section, the thermal energy as calculated by using the reported experimental values should be insufficient to explain the observed temperature variation of the physical system under examination. In order to explain such a divergence, several different factors should be taken into account and investigated:

- Correlation between the volume of GNPs and temperature (swelling effect)[2]; in our case, for sake of simplicity, we did not consider this aspect (static approximation);

- Clusters of GNPs that, due to several, different phenomena (electrostatic interaction, gravitational sedimentation, chemical adsorption, etc.) can accumulate on the glass/ITO/polyimide surfaces, which have been rubbed

for obtaining a planar orientation of the NLC director. The presence of these clusters can deeply affect the anchoring energy of the NLC molecules.

- Electron-electron scattering in the conduction band of GNPs[39];

- Plasmon-induced hot carrier generation, which can produce heat through the nonradiative decay channel[40].

At present, work is in progress with the aim of quantifying in our theoretical model the role played by each aspect (including the thermal energy production in the heat energy balance) and performing new experiments with different liquid crystalline compounds and GNPs geometries (e.g. layered GNPs).

5 Conclusion

We have reported an investigation of the nanoscale heat propagation in a system consisting of photo-excited GNPs surrounded by thermo-sensitive NLC. A theoretical model, based on the thermal heating equation, has been implemented, which takes into account the asymmetric shape of NLC molecules. Experiments have been realized by dissolving a suitable amount of GNPs in NLC. The well aligned hybrid system (NLC/GNPs) exhibits a photo-thermal sensitivity, and experimental results show a strong change in the value of the refractive index of the NLC when GNPs are photo-heated by a suitable (resonant) optical radiation. A thermographic comparison between the hybrid system and the pure NLC, carried out in the same experimental conditions, shows that the photo-thermal conversion is only due to the LPR mechanism. Theoretical predictions and experimental results exhibit a good qualitative agreement and work is in progress to introduce in the model those disregarded effects that could enable to obtain a more quantitative description of the observed phenomena. Our achievements represent a step-forward in understanding the nanoscale heat transfer in anisotropic media, which is a fundamental key-point in numerous thermal based applications of nanophotonics.

6 Acknowledgements

References

1 G. Baffou and R. Quidant, *Laser & Photonics Reviews*, 2013, **7**, 171–187.
2 A. O. Govorov and H. H. Richardson, *Nano Today*, 2007, **2**, 30–38.
3 G. Baffou, R. Quidant and C. Girard, *Applied Physics Letters*, 2009, **94**, 153109.
4 A. O. Govorov, W. Zhang, T. Skeini, H. Richardson, J. Lee and N. A. Kotov, *Nanoscale Research Letters*, 2006, **1**, 84–90.
5 X. Huang, P. K. Jain, I. H. El-Sayed and M. A. El-Sayed, *Lasers in medical science*, 2008, **23**, 217–228.
6 P. K. Jain, I. H. El-Sayed and M. A. El-Sayed, *nano today*, 2007, **2**, 18–29.
7 F. X. Gu, R. Karnik, A. Z. Wang, F. Alexis, E. Levy-Nissenbaum, S. Hong, R. S. Langer and O. C. Farokhzad, *Nano today*, 2007, **2**, 14–21.
8 S. Lal, S. E. Clare and N. J. Halas, *Accounts of chemical research*, 2008, **41**, 1842–1851.
9 P. Cherukuri, E. S. Glazer and S. A. Curley, *Advanced drug delivery reviews*, 2010, **62**, 339–345.
10 A. Vogel, J. Noack, G. Hüttman and G. Paltauf, *Applied Physics B*, 2005, **81**, 1015–1047.
11 A. Vogel and V. Venugopalan, *Chemical reviews*, 2003, **103**, 577–644.
12 G. Han, P. Ghosh, M. De and V. M. Rotello, *Nanobiotechnology*, 2007, **3**, 40–45.
13 P. Ghosh, G. Han, M. De, C. K. Kim and V. M. Rotello, *Advanced drug delivery reviews*, 2008, **60**, 1307–1315.
14 B. P. Timko, T. Dvir and D. S. Kohane, *Advanced Materials*, 2010, **22**, 4925–4943.
15 D. Boyer, P. Tamarat, A. Maali, B. Lounis and M. Orrit, *Science*, 2002, **297**, 1160–1163.
16 L. Cao, D. N. Barsic, A. R. Guichard and M. L. Brongersma, *Nano letters*, 2007, **7**, 3523–3527.
17 C. N. Baroud, J.-P. Delville, F. Gallaire and R. Wunenburger, *Physical Review E*, 2007, **75**, 046302.
18 T. Placido, E. Fanizza, P. Cosma, M. Striccoli, M. L. Curri, R. Comparelli and A. Agostiano, *Langmuir*, 2014, **30**, 2608–2618.
19 I. Ros, T. Placido, V. Amendola, C. Marinzi, N. Manfredi, R. Comparelli, M. Striccoli, A. Agostiano, A. Abbotto, D. Pedron *et al.*, *Plasmonics*, 2014, **9**, 581–593.
20 G. Baffou, P. Bon, J. Savatier, J. Polleux, M. Zhu, M. Merlin, H. Rigneault and S. Monneret, *ACS nano*, 2012, **6**, 2452–2458.
21 H. H. Richardson, Z. N. Hickman, A. O. Govorov, A. C. Thomas, W. Zhang and M. E. Kordesch, *Nano letters*, 2006, **6**, 783–788.
22 O. M. Wilson, X. Hu, D. G. Cahill and P. V. Braun, *Physical Review B*, 2002, **66**, 224301.
23 *Active Plasmonic Nanomaterials*, ed. L. De Sio, Pan Stanford, 2015.
24 L. De Sio, T. Placido, S. Serak, R. Comparelli, M. Tamborra, N. Tabiryan, M. L. Curri, R. Bartolino, C. Umeton and T. Bunning, *Advanced Optical Materials*, 2013, **1**, 899–904.
25 H. S. Carslaw and J. C. Jaeger, *Conduction of heat in solids*, Clarendon Press, 1959.
26 G. Mie, *Annalen der Physik*, 1908, **330**, 377–445.
27 C. Umeton, A. Sgrò and F. Simoni, *JOSA B*, 1987, **4**, 1938–1942.
28 L. M. Blinov, *Structure and properties of liquid crystals*, Springer, 2010, vol. 123.
29 R. Caputo, A. Veltri, C. Umeton and A. V. Sukhov, *JOSA B*, 2005, **22**, 735–742.
30 J. Li, S. Gauza and S.-T. Wu, *Journal of applied physics*, 2004, **96**, 19–24.
31 J. Li and S.-T. Wu, *Journal of applied physics*, 2004, **95**, 896–901.
32 J. Li and S.-T. Wu, *Journal of applied physics*, 2004, **96**, 170–174.
33 J. Li, C.-H. Wen, S. Gauza, R. Lu and S.-T. Wu, *Display Technology, Journal of*, 2005, **1**, 51–61.
34 G. Ahlers, D. S. Cannell, L. I. Berge and S. Sakurai, *Physical Review E*,

1994, **49**, 545.

35 P. B. Johnson and R.-W. Christy, *Physical Review B*, 1972, **6**, 4370.

36 P. Yeh, *JOSA*, 1982, **72**, 507–513.

37 N. Tabiryan, A. Sukhov and B. Y. Zel'Dovich, *Molecular Crystals and Liquid Crystals*, 1986, **136**, 1–139.

38 M. Warenghem, J. Blach and J. Henninot, *JOSA B*, 2008, **25**, 1882–1887.

39 X. Huang, S. Neretina and M. A. El-Sayed, *Advanced Materials*, 2009, **21**, 4880–4910.

40 A. Manjavacas, J. G. Liu, V. Kulkarni and P. Nordlander, *ACS nano*, 2014, **8**, 7630–7638.